

# On Model Selection Consistency of Lasso for High-Dimensional Ising Models on Tree-like Graphs

Xiangming Meng<sup>\*1</sup>, Tomoyuki Obuchi<sup>†2</sup> and Yoshiyuki Kabashima<sup>‡1</sup>

<sup>1</sup>Institute for Physics of Intelligence and Department of Physics, Graduate School of Science, The University of Tokyo, Tokyo, Japan

<sup>2</sup>Department of Systems Science, Graduate School of Informatics, Kyoto University, Kyoto, Japan

February 7, 2022

## Abstract

We consider the problem of high-dimensional Ising model selection using neighborhood-based least absolute shrinkage and selection operator (Lasso). It is rigorously proved that under some mild coherence conditions on the population covariance matrix of the Ising model, consistent model selection can be achieved with sample sizes  $n = \Omega(d^3 \log p)$  for any tree-like graph in the paramagnetic phase, where  $p$  is the number of variables and  $d$  is the maximum node degree. The obtained sufficient conditions for consistent model selection with Lasso are the same in the scaling of the sample complexity as that of  $\ell_1$ -regularized logistic regression.

## 1 Introduction

Ising model [Ising, 1925] is one renowned binary undirected graphical models (also known as Markov random fields (MRFs)) [Koller and Friedman, 2009, Mezard and Montanari, 2009, Wainwright and Jordan, 2008] with wide applications in various scientific disciplines such as social networking [McAuley and Leskovec, 2012, Perc et al., 2017], gene network analysis [Krishnan et al., 2020, Marbach et al., 2012], and protein interactions [Liebl and Zacharias, 2021, Morcos et al., 2011], just to name a few. Given an undirected graph  $G = (V, E)$ , where  $V = \{1, \dots, p\}$  is a collection of nodes associated with the binary spins  $X = (X_i)_{i=1}^p$  and

---

<sup>\*</sup>E-mail: meng@g.ecc.u-tokyo.ac.jp

<sup>†</sup>E-mail: obuchi@i.kyoto-u.ac.jp

<sup>‡</sup>E-mail: kaba@phys.s.u-tokyo.ac.jp

$E = \{(r, t) | \theta_{rt}^* \neq 0\}$  is a collection of undirected edges that specify the pairwise interactions  $\theta^* = (\theta_{rt}^*)_{r \neq t}$ , the joint probability distribution of an Ising model has the following form

$$\mathbb{P}_{\theta^*}(x) = \frac{1}{Z(\theta^*)} \exp \left\{ \sum_{r \neq t} \theta_{rt}^* x_r x_t \right\}, \quad (1)$$

where  $Z(\theta^*) = \sum_x \exp \left\{ \sum_{r \neq t} \theta_{rt}^* x_r x_t \right\}$  is the partition function. In general, there are also external fields but here they are assumed to be zero for simplicity. Importantly, the conditional independence between  $X = (X_i)_{i=1}^p$  can be well captured by the associated graph  $G$  [Koller and Friedman, 2009, Wainwright and Jordan, 2008] and hence one fundamental problem, namely Ising model selection, is to recover the underlying graph structure (edge set  $E$ ) of  $G$  from a collection of  $n$  i.i.d. samples  $\mathfrak{X}_1^n := \{x^{(1)}, \dots, x^{(n)}\}$ , where  $x^{(i)} \in \{-1, +1\}^p$  represents the  $i$ -th sample. To address this fundamental problem, a variety of methods have been proposed over the past several decades in various fields [Decelle and Ricci-Tersenghi, 2014, Höfling and Tibshirani, 2009, Kappen and Rodríguez, 1998, Lokhov et al., 2018, Ravikumar et al., 2010, Ricci-Tersenghi, 2012, Tanaka, 1998, Vuffray et al., 2016, Wainwright et al., 2007]. Notably, under the framework of the pseudo-likelihood (PL) [Besag, 1975], both  $\ell_1$ -regularized logistic regression ( $\ell_1$ -LogR) [Ravikumar et al., 2010] and  $\ell_1$ -regularized interaction screening estimator (RISE) [Lokhov et al., 2018, Vuffray et al., 2016] have become the two most popular methods in reconstructing the graph structure and the number of samples required is even near-optimal with respect to (w.r.t.) previously established information-theoretic lower-bound [Santhanam and Wainwright, 2012], especially at low temperatures.

In this paper, we consider the simple and well-known least absolute shrinkage and selection operator (Lasso) [Tibshirani, 1996] for Ising model selection. At first sight, one might even doubt its suitability for this problem since apparently the Ising snapshots are binary data generated in a nonlinear manner while Lasso is (presumably) used for continuous data with linear regression. In fact, the idea of using linear regression for binary data is not as outrageous (or naive) as one might imagine [Brillinger, 1982], and perhaps surprisingly, sometimes linear regression even outperforms logistic regression as demonstrated in [Gomila, 2021]. Indeed, if our goal is to make predictions of new outcomes, say binary classification, then linear regression is clearly not a good choice since it is easily prone to out-of-bound forecasts. However, when it comes to other goals such as estimating variables or causal effects [Gomila, 2021], the answer becomes highly nontrivial. For Ising model selection, the goal is not about making predictions of new binary outcomes, but inferring the graph structure and thus deciphering the underlying conditional independence between different variables. Hence, given the popularity of Lasso, it is of both practical and theoretical significance to study the (mis-specified) Lasso’s *model selection consistency* for the nonlinear Ising models, i.e., under what conditions Lasso can (or cannot) successfully recover the true structure of Ising model. While several early studies [Bento and Montanari, 2009, Lokhov et al., 2018, Meng et al., 2020, 2021] have already suggested Lasso’s potential

consistency for Ising model selection under specific cases, a rigorous theoretical analysis has still remained largely unresolved.

Here, as in Ravikumar et al. [2010], we consider the slightly stronger criterion of *signed edge* recovery, and investigates the sufficient conditions on the *sparsistency property* of Lasso.

**Definition 1** (*signed edge Ravikumar et al. [2010]*) Given one Ising model  $G = (V, E)$  with interactions  $\theta^*$ , the signed edge set  $E^*$  is defined as  $E^* := \{\text{sign}(\theta_{rt}^*)\}$  where  $\text{sign}(\cdot)$  is an element-wise operation that maps every positive entry to 1, negative entry to -1, and zero entry to zero.

**Definition 2** (*sparsistency property [Ravikumar et al., 2010]*) Suppose that  $\hat{E}_n$  is an estimator of the signed edge  $E^*$  given  $\mathfrak{X}_1^n$ , then it is called (*signed*) *model selection consistent* in the sense that

$$\mathbb{P}\left(\hat{E}_n = E^*\right) \rightarrow 1 \text{ as } n \rightarrow +\infty, \quad (2)$$

which is also known as the *sparsistency property*.

The goal is to investigate the sufficient conditions when Lasso is *model selection consistent* for high dimensional Ising models.

## 1.1 Our Contributions

In this paper, we theoretically analyze the model selection consistency of Lasso for Ising models. The high dimensional ( $n \ll p$ ) regime is considered, where both the number of vertices  $p = p(n)$  and the maximum node degree  $d = d(n)$  may also scale as a function of the sample size  $n$ . Our main contributions are as follows.

Generally, we prove that for high-dimensional Ising models on any tree-like graphs in the whole paramagnetic phase, i.e., the spontaneous magnetization of Ising model is zero [Mezard and Montanari, 2009, Nishimori, 2001], the mis-specified lasso estimator is still model selection consistent, and remarkably, the required sample complexity has the same scaling as that of  $\ell_1$ -LogR. Specifically, we show that under mild assumptions on the population covariance matrix, consistent Ising model selection can be achieved using  $\Omega(d^3 \log p)$  samples with Lasso. When the same assumptions are directly imposed on the sample covariance matrices, only  $\Omega(d^2 \log p)$  samples suffice. Compared to previous works [Lokhov et al., 2018, Meng et al., 2021], we provide a rigorous analysis of Lasso for Ising model selection and explicitly prove its consistency in the whole paramagnetic phase. Given the wide popularity and efficiency of Lasso, such rigorous analysis provides a theoretical backing for its practical use in Ising model selection, which can also be viewed as a complement to that for Gaussian graphical models [Meinshausen et al., 2006, Zhao and Yu, 2006].

## 1.2 Related Works

In Bento and Montanari [2009], the authors pointed out a potential relevance of the incoherence condition of Lasso [Zhao and Yu, 2006] to  $\ell_1$ -LogR by expanding the logistic loss

around the true interactions  $\theta^*$ . However, on the one hand, it is restricted to the case when the  $\ell_1$  regularization parameter approaches zero. On the other hand, the resultant quadratic loss is actually different from that of Lasso. Later, Lokhov et al. [2018] observed that at high temperatures when the magnitude of interactions approaches zero, both the logistic and IOS losses can be approximated as a square loss using a second-order Taylor expansion around zero (as opposed to  $\theta^*$  in Zhao and Yu [2006]). However, without considering the  $\ell_1$  regularization term, Lokhov et al. [2018] simply compared the analytical solution with that of the naive mean-field method [Kappen and Rodríguez, 1998, Ricci-Tersenghi, 2012, Tanaka, 1998]. A rigorous theoretical analysis of the Lasso estimator itself is still lacking. In other words, although Taylor expansion is used in Bento and Montanari [2009], Lokhov et al. [2018] to illustrate the potential similarity between Lasso and  $\ell_1$ -LogR/RISE, there is no quantitative analysis of the exact valid regime for the consistency of Lasso as well as the corresponding sufficient conditions including the sample complexity.

To the best of our knowledge, the first explicit analysis of Lasso for Ising model selection is given in Meng et al. [2021] using statistical physics methods, building on previous studies [Abbara et al., 2020, Bachschmid-Romano and Opper, 2017, Meng et al., 2020]. In particular, Meng et al. [2021] demonstrated that Lasso has the same order of sample complexity as  $\ell_1$ -LogR for random regular (RR) graphs in the paramagnetic phase [Mezard and Montanari, 2009]. Furthermore, Meng et al. [2021] provided an accurate estimate of the typical sample complexity as well as a precise prediction of the non-asymptotic learning performance. However, there are several limitations in Meng et al. [2021]. First, since the replica method [Mezard and Montanari, 2009, Nishimori, 2001, Opper and Saad, 2001] they use is a non-rigorous method from statistical mechanics, a rigorous mathematical proof is lacking. Second, the results in Meng et al. [2021] are restricted to the ensemble of RR graphs. In addition, since their analysis relies on the *self averaging property* [Mezard and Montanari, 2009, Nishimori, 2001], the results in Meng et al. [2021] are meaningful in terms of the “typical case” [Engel and Van den Broeck, 2001] rather than the worst case.

Regarding the study of Lasso for nonlinear (not necessarily binary) targets, the past few years have seen an active line of research in the field of signal processing with a special focus on the single-index model [Brillinger, 1982, Genzel, 2016, Plan and Vershynin, 2016, Thrampoulidis et al., 2015, Zhang et al., 2016]. These studies are related to ours but with several important differences. First, in our study, the covariates are generated from an Ising model rather than a Gaussian distribution. Second, we focus on model selection consistency of Lasso while most previous studies considered estimation consistency except Zhang et al. [2016]. However, Zhang et al. [2016] only considered the classical asymptotic regime while we are interested in the high-dimensional setting where  $n \ll p$ .

### 1.3 Notations and Organizations

For each vertex  $r \in V$ , the neighborhood set is denoted as  $\mathcal{N}(r) := \{t \in V \mid (r, t) \in E\}$ , the signed neighborhood set is defined as  $\mathcal{N}_{\pm}(r) := \{\text{sign}(\theta_{rt}^*) t \mid t \in \mathcal{N}(r)\}$ , and the corresponding node degree is denoted as  $d_r := |\mathcal{N}(r)|$ . The maximum node degree of the whole

graph  $G$  is denoted as  $d := \max_{r \in V} d_r$ . We use  $\mathcal{G}_{p,d}$  to denote the ensemble of graphs  $G$  with  $p$  vertices and maximum (not necessarily bounded) node degree  $d \geq 3$ . The minimum and maximum magnitudes of the interactions  $\theta_{rt}^*$  for  $(r,t) \in E$  are respectively denoted as

$$\theta_{\min}^* := \min_{(r,t) \in E} |\theta_{rt}^*|, \quad \theta_{\max}^* := \max_{(r,t) \in E} |\theta_{rt}^*|. \quad (3)$$

The  $\ell_1$ -norm of a vector  $a$  is denoted as  $\|a\|_1$ .  $\mathbb{E}_{\theta^*} \{\cdot\}$  denotes expectation w.r.t. the joint distribution  $\mathbb{P}_{\theta^*}(x)$  (1).  $\|A\|_\infty = \max_j \sum_k |A_{jk}|$  is the  $\ell_\infty$  matrix norm of a matrix  $A$ .  $\Lambda_{\min}(A)$  and  $\Lambda_{\max}(A)$  denote the minimum and maximum eigenvalue of  $A$ , respectively.

The remainder of this paper is organized as follows. In section 2, we provide the problem setup. Section 3 states the main results. Section 4 gives the proof of the main results. In Section 5, numerical simulations are conducted to verify the theoretical analysis. Finally, Section 6 concludes the paper with some discussions.

## 2 Problem Setup

For any graph  $G = (V, E)$ , recovering the signed edge  $E^*$  is equivalent to reconstructing the associated neighborhood set  $\mathcal{N}(r)$  for each vertex  $r \in V$  along with its correct signs  $\text{sign}(\theta_{rt}^*) \forall t \in \mathcal{N}(r)$  [Ravikumar et al., 2010]. As a result, similar to  $\ell_1$ -LogR and RISE, we consider the neighborhood based approach for Lasso. Specifically,  $\forall r \in V$ , the estimate of the sub-vector  $\theta_{\setminus r}^* := \{\theta_{rt}^* | t \in V \setminus r\} \in \mathbb{R}^{p-1}$  is obtained by Lasso as

$$\hat{\theta}_{\setminus r} = \arg \min_{\theta_{\setminus r}} \left\{ \ell(\theta_{\setminus r}; \mathfrak{X}_1^n) + \lambda_{(n,p,d)} \|\theta_{\setminus r}\|_1 \right\}, \quad (4)$$

where  $\ell(\theta_{\setminus r}; \mathfrak{X}_1^n)$  denotes the square loss function

$$\ell(\theta_{\setminus r}; \mathfrak{X}_1^n) := \frac{1}{2n} \sum_{i=1}^n (x_r^{(i)} - \sum_{u \in V \setminus r} \theta_{ru} x_u^{(i)})^2, \quad (5)$$

and  $\lambda_{(n,p,d)} > 0$  is the regularization parameter, which might depend on the value of  $(n, p, d)$ . For notational simplicity, instead of  $\lambda_{(n,p,d)}$ ,  $\lambda_n$  will be used hereafter. Then, given  $\hat{\theta}_{\setminus r}$ , the estimated signed neighborhood of  $\mathcal{N}_\pm(r)$ , denoted as  $\hat{\mathcal{N}}_\pm(r)$ , can be obtained as follows

$$\hat{\mathcal{N}}_\pm(r) := \left\{ \text{sign}(\hat{\theta}_{rt}) t | t \in V \setminus r, \hat{\theta}_{rt} \neq 0 \right\}. \quad (6)$$

Consequently, the event  $\{\hat{E}_n = E^*\}$  is equivalent to the event  $\{\hat{\mathcal{N}}_\pm(r) = \mathcal{N}_\pm(r), \forall r \in V\}$ , i.e., every signed neighborhood set is recovered correctly. Our main concern is the scaling condition on  $(n, p, d)$  which ensures that the estimated signed neighborhood  $\hat{\mathcal{N}}_\pm(r)$  in (6) agrees with the true neighborhood, i.e.,  $\{\hat{\mathcal{N}}_\pm(r) = \mathcal{N}_\pm(r), \forall r \in V\}$ , with high probability.

### 3 Main results

#### 3.1 Assumptions

**Assumption 1 (A1):** *Paramagnetic tree-like graph.* The graph  $G \in \mathcal{G}_{p,d}$  of the Ising model is assumed to be a sparse tree graph in the paramagnetic phase [Mezard and Montanari, 2009].

The paramagnetic phase means that the Ising model is above the critical temperature so that the spontaneous magnetization is zero [Mezard and Montanari, 2009, Nishimori, 2001]. While it is used in our proof of the main results, it is conjectured that assumption (A1) can be further relaxed. In fact, the experiments in Section 5 imply that, even for graphs with many loops, the reconstruction probability of Lasso behaves essentially similarly as  $\ell_1$ -LogR. We here leave relaxing assumption (A1) as an important future work.

In Ravikumar et al. [2010], two additional conditions, namely *dependency condition* and *incoherence condition*, are assumed. In the case of Lasso,  $\forall r \in V$ , as opposed to Ravikumar et al. [2010], the Hessian of  $\mathbb{E}_{\theta^*} \{\ell(\theta; \mathfrak{X}_1^n)\}$  reduces to the covariance matrix, i.e.,

$$Q_r^* := \mathbb{E}_{\theta^*} \{\nabla^2 \ell(\theta; \mathfrak{X}_1^n)\} = \mathbb{E}_{\theta^*} \{X_{\setminus r} X_{\setminus r}^T\}. \quad (7)$$

For notational simplicity,  $Q_r^*$  will be written as  $Q^*$  hereafter. Denote  $S := \{(r, t) \mid t \in \mathcal{N}(r)\}$  as the subset of indices associated with edges of  $r$  and  $S^c$  as its complement. The  $d_r \times d_r$  sub-matrix of  $Q^*$  indexed by  $S$  is denoted as  $Q_{SS}^*$ . Other sub-matrices like  $Q_{S^c S}^*$  are defined in the same way.

**Condition 1 (C1):** *dependency condition.* The sub-matrix  $Q_{SS}^*$  has bounded eigenvalue, i.e., there exists a constant  $C_{\min} > 0$  such that

$$\Lambda_{\min}(Q_{SS}^*) \geq C_{\min}. \quad (8)$$

Moreover, it is required that  $\Lambda_{\max}(Q^*) \leq D_{\max}$ .

**Condition 2 (C2):** *incoherence condition.* There exists an  $\alpha \in (0, 1]$  such that

$$\| \| Q_{S^c S}^* (Q_{SS}^*)^{-1} \| \|_{\infty} \leq 1 - \alpha. \quad (9)$$

Interestingly, in the special case of RR graphs, we have Proposition 1 while it is conjectured to also hold for general graphs under assumption (A1).

**Proposition 1** *For RR graphs, both the dependency condition (C1) and incoherence condition (C2) naturally hold under the assumption (A1).*

**Proof** See D.1. ■

### 3.2 Statement of main results

We are now ready to state our main result, as shown in Theorem 1.

**Theorem 1** *Consider an Ising model defined on a graph  $G = (V, E) \in \mathcal{G}_{p,d}$  with parameter vector  $\theta^*$  and associated signed edge set  $E^*$  such that assumption (A1) is satisfied. Moreover, conditions (C1) and (C2) are satisfied by the population covariance matrix  $Q^*$ . Suppose that the regularization parameter  $\lambda_n$  is selected to satisfy  $\lambda_n \geq \frac{4\sqrt{c+1}(2-\alpha)}{\alpha} \sqrt{\frac{\log p}{n}}$  for some constant  $c > 0$ . Then there exists a constant  $L$  independent of  $(n, p, d)$  such that if*

$$n \geq Ld^3 \log p, \tag{10}$$

then with probability at least  $1 - 2\exp(-c \log p) \rightarrow 1$  as  $p \rightarrow \infty$ , the following properties hold:

(a) For each node  $r \in V$ , the Lasso estimator (4) has a unique solution, and thus uniquely specifies a signed neighborhood  $\hat{N}_\pm(r)$ .

(b) For each node  $r \in V$ , the estimated signed neighborhood vector  $\hat{N}_\pm(r)$  correctly excludes all edges not in the true neighborhood. Moreover, it correctly includes all edges if the minimum magnitude of the rescaled parameter satisfies  $\tilde{\theta}_{\min}^* \geq \frac{6\lambda_n \sqrt{d}}{C_{\min}}$ .

Theorem 1 indicates that the probability that Lasso recovers the true signed edge set approaches one exponentially as a function of  $\log p$ . Hence, under conditions (C1) and (C2), in the high-dimensional setting (for  $p \rightarrow \infty$ ), Lasso is model selection consistent with  $n = \Omega(d^3 \log p)$  samples, same as  $\ell_1$ -LogR, for any tree-like Ising models in the paramagnetic phase. Moreover, in the special case of RR graphs, Proposition 1 implies that the same conclusion holds without additional requirement of conditions (C1) and (C2), which is consistent with the result in Meng et al. [2021].

## 4 Proof of the Main Results

In this section, we present the detailed proofs of the main results.

### 4.1 Sketch of the proof

First of all, assuming both conditions (C1) and (C2) are directly imposed on the sample covariance matrices  $Q^n := \frac{1}{n} \sum_{i=1}^n x_{\setminus r}^{(i)} \left(x_{\setminus r}^{(i)}\right)^T$ , we prove Proposition 2 in such a “fixed design” case:

**Proposition 2** (*fixed design*) *Consider an Ising model defined on a graph  $G = (V, E) \in \mathcal{G}_{p,d}$  with parameter vector  $\theta^*$  and associated signed edge set  $E^*$  such that the assumption (A1) is satisfied. Suppose that the sample covariance  $Q^n$  satisfies (C1) and (C2) and the*

regularization parameter  $\lambda_n$  satisfies  $\lambda_n \geq \frac{4\sqrt{c+1}(2-\alpha)}{\alpha} \sqrt{\frac{\log p}{n}}$  for some constant  $c > 0$ . Under these conditions, if

$$n \geq (c+1)d^2 \log p, \quad (11)$$

then with probability at least  $1 - 2 \exp(-c \log p) \rightarrow 1$  as  $p \rightarrow \infty$ , the following properties hold:

(a) For each node  $r \in V$ , the Lasso estimator (4) has a unique solution, and thus uniquely specifies a signed neighborhood  $\hat{N}_{\pm}(r)$ .

(b) For each node  $r \in V$ , the estimated signed neighborhood vector  $\hat{N}_{\pm}(r)$  correctly excludes all edges not in the true neighborhood. Moreover, it correctly includes all edges if  $\tilde{\theta}_{\min}^* \geq \frac{6\lambda_n \sqrt{d}}{C_{\min}}$ , where  $\tilde{\theta}_{\min}^*$  is the minimum magnitude of the rescaled parameter  $\tilde{\theta}^*$  which is defined later in (16).

Then, it is demonstrated that imposing the same conditions on the population covariance matrices  $Q_r^*$  guarantees that the associated conditions hold for the sample covariance matrices  $Q^n$  with high probability, which leads to the proof of Theorem 1. Given Proposition 2, the proof of Theorem 1 is the same as that of Ravikumar et al. [2010] using some large-deviation analysis and thus our main focus is on the proof of Proposition 2.

We use the primal-dual witness proof framework [Ravikumar et al., 2010], which was originally proposed in Wainwright [2009]. The main idea of the primal-dual witness method is to explicitly construct an optimal primal-dual pair which satisfies the sub-gradient optimality conditions associated with the Lasso estimator (4). Subsequently, we prove that under the stated assumptions on  $(n, p, d)$ , the optimal primal-dual pair can be constructed such that they act as a witness, i.e., a certificate that guarantees that the neighborhood-based Lasso estimator correctly recovers the signed edge set of the graph  $G \in \mathcal{G}_{p,d}$ .

Specifically, for each vertex  $r \in V$ , an optimal primal-dual pair  $(\hat{\theta}_{\setminus r}, \hat{z}_r)$  is constructed, where  $\hat{\theta}_{\setminus r} \in \mathbb{R}^{p-1}$  is a primal solution and  $\hat{z}_r \in \mathbb{R}^{p-1}$  is the associated sub-gradient vector. They satisfy the zero sub-gradient optimality condition [Rockafellar, 1970] associated with Lasso (4):

$$\nabla \ell(\hat{\theta}_{\setminus r}; \mathbf{x}_1^n) + \lambda_n \hat{z}_r = 0, \quad (12)$$

where the sub-gradient vector  $\hat{z}_r$  satisfies

$$\begin{cases} \hat{z}_{rt} = \text{sign}(\hat{\theta}_{rt}), \text{ if } \hat{\theta}_{rt} \neq 0; & (a) \\ |\hat{z}_{rt}| \leq 1, \text{ otherwise.} & (b) \end{cases} \quad (13)$$

Then, the pair is a primal-dual optimal solution to (4) and its dual. Further, to ensure that such an optimal primal-dual pair correctly specifies the signed neighborhood of node  $r$ , the



sufficient and necessary conditions are as follows

$$\begin{cases} \text{sign}(\hat{z}_{rt}) = \text{sign}(\theta_{rt}^*), \forall (r, t) \in S := \{(r, t) \mid (r, t) \in E\}, & (a) \\ \hat{\theta}_{ru} = 0, \forall (r, u) \in S^c := E \setminus S. & (b) \end{cases} \quad (14)$$

Note that while the regression in (4) corresponds to a convex problem, for  $p \gg n$  in the high-dimensional regime, it is not necessarily strictly convex so that there might be multiple optimal solutions. Fortunately, the following lemma in Ravikumar et al. [2010] provides sufficient conditions for shared sparsity among optimal solutions as well as uniqueness of the optimal solution.

**Lemma 1** (Lemma 1 in Ravikumar et al. [2010]). *Suppose that there exists an optimal primal solution  $\hat{\theta}_{\setminus r}$  with associated optimal dual vector  $\hat{z}_r$  such that  $\|\hat{z}_{S^c}\|_\infty < 1$ . Then any optimal primal solution  $\tilde{\theta}$  must have  $\tilde{\theta}_{S^c} = 0$ . Moreover, if the Hessian sub-matrix  $[\nabla^2 \ell(\hat{\theta}_{\setminus r}; \mathfrak{X}_1^n)]_{SS}$  is strictly positive definite, then  $\hat{\theta}_{\setminus r}$  is the unique optimal solution.*

Thus, we can construct a primal-dual witness  $(\hat{\theta}_r, \hat{z})$  for the Lasso estimator (4) as follows:

- (a) First, set  $\hat{\theta}_S$  as the minimizer of the partial penalized likelihood

$$\hat{\theta}_S = \arg \min_{\theta_{\setminus r} = (\theta_S, 0) \in \mathbb{R}^{p-1}} \{\ell(\theta_{\setminus r}; \mathfrak{X}_1^n) + \lambda_n \|\theta_S\|_1\}, \quad (15)$$

and then set  $\hat{z}_S = \text{sign}(\hat{\theta}_S)$ .

- (b) Second, set  $\hat{\theta}_{S^c} = 0$  so that condition (14) (b) holds.

- (c) Third, obtain  $\hat{z}_{S^c}$  from (12) by substituting the values of  $\hat{\theta}_{\setminus r}$  and  $\hat{z}_S$ .

- (d) Finally, we need to show that the stated scalings of  $(n, p, d)$  imply that, with high probability, the remaining conditions (13) and (14) (a) are satisfied.

## 4.2 A comparison with the proof of $\ell_1$ -LogR in Ravikumar et al. [2010]

Before going into details of the proof, we briefly compare it to that for  $\ell_1$ -LogR in Ravikumar et al. [2010]. While both proofs build on the same primal-dual witness framework [Wainwright, 2009] and share some similarities, there are two crucial differences due to the different loss functions of Lasso and  $\ell_1$ -LogR. First, the solution to the zero-gradient condition  $\mathbb{E}_{\theta^*} \{\ell(\theta; \mathfrak{X}_1^n)\} = 0$  is no longer the true parameter vector but a rescaled one (see Lemma 2). Second, the Hessian matrix of  $\mathbb{E}_{\theta^*} \{\ell(\theta; \mathfrak{X}_1^n)\}$  corresponds to the covariance matrix of  $X_{\setminus r}$ , which is independent of the value of  $\theta$  and hence the additional variance function term in Ravikumar et al. [2010] does not exist. Interestingly, such differences on the one hand simplify the analysis somewhere (Lemma 5) while on the other hand complicate the analysis elsewhere (Lemma 2, 3, 4) but overall, remarkably, it leads to the same scaling of the sample complexity as  $\ell_1$ -LogR [Ravikumar et al., 2010] for consistent Ising model selection.

### 4.3 Some key results

Some key technical results central to the main proof are presented in this subsection. First, we obtain the zero-gradient solution to  $\mathbb{E}_{\theta^*} (\nabla \ell (\theta_{\setminus r}; \mathfrak{X}_1^n)) = 0$  for the square loss (5).

**Lemma 2** *For a tree graph in the paramagnetic phase (assumption (A1)), the solution to the zero-gradient condition  $\mathbb{E}_{\theta^*} (\nabla \ell (\theta_{\setminus r}; \mathfrak{X}_1^n)) = 0$ , denoted as  $\tilde{\theta}_{\setminus r}^* = \left\{ \tilde{\theta}_{rt}^* \right\}_{t \in V \setminus r} \in \mathbb{R}^{p-1}$ , is*

$$\tilde{\theta}_{rt}^* = \begin{cases} \frac{1}{1-d_r + \sum_{u \in \mathcal{N}(r)} \frac{1}{1-\tanh^2(\theta_{ru}^*)}} \frac{\tanh(\theta_{rt}^*)}{1-\tanh^2(\theta_{rt}^*)} & \text{if } (r, t) \in E; \\ 0 & \text{otherwise.} \end{cases} \quad (16)$$

**Proof** See Appendix A. ■

Lemma 2 indicates that, under the assumption (A1), the solution  $\tilde{\theta}_{\setminus r}^*$  shares the same sign structure as the true parameter  $\theta_{\setminus r}^*$ , i.e.,  $\text{sign}(\tilde{\theta}_{\setminus r}^*) = \text{sign}(\theta_{\setminus r}^*)$ , which is the key to the success of Lasso. The minimum magnitude of the rescaled value  $\tilde{\theta}_{rt}^*$  for  $(r, t) \in E$  is denoted as

$$\tilde{\theta}_{\min}^* := \min_{(r,t) \in E} \tilde{\theta}_{rt}^*, \quad (17)$$

where  $\tilde{\theta}_{rt}^*$  is defined in (16).

Subsequently,  $\forall r \in V$ , given  $\tilde{\theta}_{\setminus r}^*$ , we re-write the zero-subgradient condition (12) as follows

$$\nabla \ell (\hat{\theta}_{\setminus r}; \mathfrak{X}_1^n) - \nabla \ell (\tilde{\theta}_{\setminus r}^*; \mathfrak{X}_1^n) = W^n - \lambda_n \hat{z}, \quad (18)$$

where  $W^n = -\nabla \ell (\tilde{\theta}_{\setminus r}^*; \mathfrak{X}_1^n)$  are evaluated at the rescaled  $\tilde{\theta}_{\setminus r}^*$  in (16), as opposed to the true parameter  $\theta_{\setminus r}^*$  [Ravikumar et al., 2010]. Using the mean-value theorem element-wise to (18) yields

$$\nabla^2 \ell (\tilde{\theta}_{\setminus r}^*; \mathfrak{X}_1^n) [\hat{\theta}_{\setminus r} - \tilde{\theta}_{\setminus r}^*] = W^n - \lambda_n \hat{z}. \quad (19)$$

In contrast to Ravikumar et al. [2010], the remainder term disappears due to the square loss (5). The  $s$ -th element of  $W^n$ , denoted as  $W_s^n$ , can be written as follows

$$W_s^n = \frac{1}{n} \sum_{i=1}^n Z_s^{(i)}, \quad \forall s \in V \setminus r, \quad (20)$$

$$Z_s^{(i)} := x_s^{(i)} \left( x_r^{(i)} - \sum_{t \in V \setminus r} \tilde{\theta}_{rt}^* x_t^{(i)} \right). \quad (21)$$

It can be seen that  $W^n$  has a quite different form and thus behaves differently from the result in Ravikumar et al. [2010]. The properties of the random variable  $Z_s^{(i)}$  are shown in Lemma 3.

**Lemma 3** *The random variable  $Z_s^{(i)}$  defined in (21) has zero mean and bounded variance, i.e.,  $\mathbb{E}_{\theta^*} \left( Z_s^{(i)} \right) = 0$ ,  $\text{Var} \left( Z_s^{(i)} \right) \leq 1$ . Furthermore,  $Z_s^{(i)}$  itself is bounded by  $\left| Z_s^{(i)} \right| \leq d$ .*

**Proof** See Appendix B. ■

Using the results in Lemma 3, we obtain the behavior of  $\|W^n\|_\infty$  as follows.

**Lemma 4** *For the specified mutual incoherence parameter  $\alpha \in (0, 1]$ , if  $n \geq (c + 1) d^2 \log p$  for some constant  $c > 0$  and  $\lambda_n \geq \frac{4\sqrt{c+1}(2-\alpha)}{\alpha} \sqrt{\frac{\log p}{n}}$ , then*

$$\mathbb{P} \left( \frac{2-\alpha}{\lambda_n} \|W^n\|_\infty \geq \frac{\alpha}{2} \right) \leq 2 \exp(-c \log p), \quad (22)$$

which converges to zero at rate  $\exp(-c \log p)$  as  $p \rightarrow +\infty$ .

**Proof** See Appendix C. ■

Moreover, it is proved that the sub-vector  $\hat{\theta}_S$  is an  $\ell_2$ -consistent estimate of the rescaled sub-vector  $\tilde{\theta}_S^*$ , as opposed to the original  $\theta_S^*$  in Ravikumar et al. [2010], as stated in Lemma 5:

**Lemma 5** ( *$\ell_2$ -consistency of the primal sub-vector*). *If  $\|W^n\|_\infty \leq \frac{\lambda_n}{2}$ , then there is*

$$\left\| \hat{\theta}_S - \tilde{\theta}_S^* \right\|_2 \leq \frac{3}{C_{\min}} \lambda_n \sqrt{d}. \quad (23)$$

**Proof** See Appendix D. ■

#### 4.4 Proof of Proposition 2

From Lemma 4, when  $n \geq (c + 1) d^2 \log p$ , if the regularization parameter is chosen to satisfy  $\lambda_n \geq \frac{4\sqrt{c+1}(2-\alpha)}{\alpha} \sqrt{\frac{\log p}{n}}$ , then it is guaranteed that with probability greater than  $1 - 2 \exp(-c \log p)$  ( $\rightarrow 1$  in the high dimensional setting for  $p \rightarrow \infty$ ), we have

$$\|W^n\|_\infty \leq \frac{\alpha}{2-\alpha} \frac{\lambda_n}{2} \leq \frac{\lambda_n}{2}, \quad (24)$$

where  $0 < \alpha \leq 1$  is used in the last inequality, so that the condition in Lemma 5 is also satisfied. The zero-subgradient condition (19) can be equivalently re-written as follows

$$\begin{cases} Q_{S^c S}^n \left( \hat{\theta}_S - \tilde{\theta}_S^* \right) = W_{S^c}^n - \lambda_n \hat{z}_{S^c}, \\ Q_{SS}^n \left( \hat{\theta}_S - \tilde{\theta}_S^* \right) = W_S^n - \lambda_n \hat{z}_S, \end{cases} \quad (25)$$

where we have used the fact that  $\hat{\theta}_{S^c} = 0$  from the primal-dual construction. After some simple algebra, we obtain

$$W_{S^c}^n - Q_{S^c S}^n (Q_{SS}^n)^{-1} W_S^n + \lambda_n Q_{S^c S}^n (Q_{SS}^n)^{-1} \hat{z}_S = \lambda_n \hat{z}_{S^c}. \quad (26)$$

For strict dual feasibility, from (26), using the triangle inequality and the mutual incoherence bound, we have

$$\begin{aligned} \|\hat{z}_{S^c}\|_\infty &\leq \|Q_{S^c S}^* (Q_{SS}^*)^{-1}\|_\infty \left[ \frac{\|W_S^n\|_\infty}{\lambda_n} + 1 \right] + \frac{\|W_{S^c}^n\|_\infty}{\lambda_n} \\ &\leq (1 - \alpha) + (2 - \alpha) \frac{\|W^n\|_\infty}{\lambda_n} \\ &\leq (1 - \alpha) + (2 - \alpha) \frac{1}{2 - \alpha} \frac{\alpha}{2} \\ &= 1 - \frac{\alpha}{2} < 1, \end{aligned} \quad (27)$$

with probability converging to one. For correct sign recovery, it suffices to show that  $\|\hat{\theta}_S - \tilde{\theta}_S^*\|_\infty \leq \frac{\tilde{\theta}_{\min}^*}{2}$ . From Lemma 5 (since (24) holds), we have

$$\frac{2}{\tilde{\theta}_{\min}^*} \|\hat{\theta}_S - \tilde{\theta}_S^*\|_\infty \leq \frac{2}{\tilde{\theta}_{\min}^*} \|\hat{\theta}_S - \tilde{\theta}_S^*\|_2 \leq \frac{6}{\tilde{\theta}_{\min}^* C_{\min}} \lambda_n \sqrt{d}. \quad (28)$$

As a result, if  $\tilde{\theta}_{\min}^* \geq \frac{6\lambda_n \sqrt{d}}{C_{\min}}$ , or  $\lambda_n \leq \frac{\tilde{\theta}_{\min}^* C_{\min}}{6\sqrt{d}}$ , the condition  $\|\hat{\theta}_S - \tilde{\theta}_S^*\|_\infty \leq \frac{\tilde{\theta}_{\min}^*}{2}$  holds.

#### 4.5 Proof of Theorem 1

Given Proposition 2, the proof of Theorem 1 is straightforward following the same line in Ravikumar et al. [2010]. For completeness, we restate the associated results in Ravikumar et al. [2010] without giving the proofs. In the case of Lasso, different from Ravikumar et al. [2010], only the covariance matrix is concerned and thus we simply need to focus on the covariance matrix.

**Lemma 6** (Lemma 5 in Ravikumar et al. [2010]) *If the dependency condition (C1) holds for the population covariance  $Q^*$ , then for any  $\delta > 0$ , there are some positive constants  $A$  and  $B$*

$$\mathbb{P} \left( \Lambda_{\max} \left( \frac{1}{n} \sum_i x_{\setminus r}^{(i)} (x_{\setminus r}^{(i)})^T \right) \geq D_{\max} + \delta \right) \leq 2 \exp \left( -A \frac{\delta^2 n}{d^2} + B \log d \right), \quad (29)$$

$$\mathbb{P} (\Lambda_{\min} (Q_{SS}^n) \leq C_{\min} - \delta) \leq 2 \exp \left( -A \frac{\delta^2 n}{d^2} + B \log d \right). \quad (30)$$

The following lemma is the analog for the incoherence condition (C2), showing that the scaling of  $(n, p, d)$  guarantees that the population incoherence implies sample incoherence.

**Lemma 7** (Lemma 6 in Ravikumar et al. [2010]) *If the incoherence condition (9) holds for the population covariance  $Q^*$ , then the sample covariance matrix satisfies an analogous version, with high probability in the sense that*

$$\mathbb{P}\left(\|Q_{S^c S}^n (Q_{SS}^n)^{-1}\|_\infty \geq 1 - \frac{\alpha}{2}\right) \leq 2 \exp\left(-K \frac{n}{d^3} + \log p\right), \quad (31)$$

where  $K > 0$  is some constant.

Consequently, if the population covariance matrix  $Q^*$  satisfies conditions (C1) and (C2), then analogous bounds hold for the sample covariance matrix  $Q^n$  and thus we can obtain Theorem 1 by combining Proposition 2 with Lemma 6 and Lemma 7 as Ravikumar et al. [2010].

## 5 Experimental Results

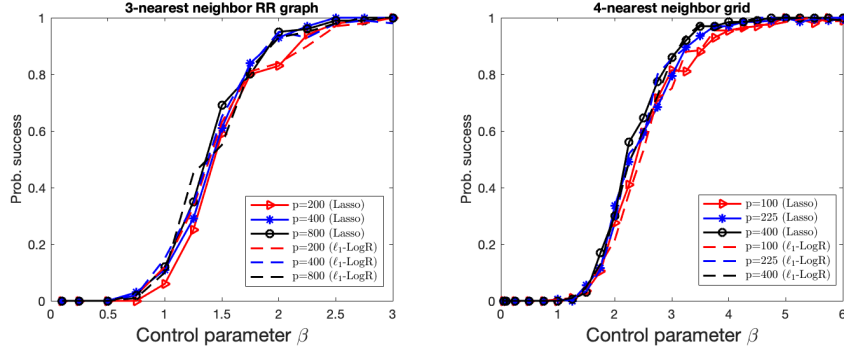


Figure 1: Success probability versus the control parameter  $\beta$  for Ising models. Left: 3-nearest neighbor RR graph with  $d = 3$  and mixed interactions  $\theta_{rt}^* = \pm 0.4$  for all  $(r, t) \in E$ ,  $\beta = \frac{n}{10d \log p}$ ; Right: 4-nearest neighbor grid graph with  $d = 4$  and positive interactions  $\theta_{rt}^* = 0.2$  for all  $(r, t) \in E$ ,  $\beta = \frac{n}{15d \log p}$ .

In this section we conduct simulations to verify our theoretical analysis. Both RR and star-shaped graphs are evaluated, representing the bounded node degree case and unbounded node degree case, respectively. In addition, as an example of graphs with many loops, we also evaluate square lattice (grid) graphs with periodic boundary condition. The experimental procedures are as follows. First, a graph  $G = (V, E) \in \mathcal{G}_{p,d}$  is generated and the Ising model is defined on it. Then, the spin snapshots are obtained using Monte-Carlo sampling, yielding the dataset  $\mathfrak{X}_1^n$ . The regularization parameter is set to be a constant factor of  $\sqrt{\frac{\log p}{n}}$ . For any graph, we performed simulations using neighborhood-based Lasso (4)  $\forall r \in V$  and then the associated signed neighborhood  $\hat{\mathcal{N}}_{\pm}(r)$  is estimated as (6). Similar to Ravikumar et al. [2010], the sample size  $n$  scaling is set to be proportional to  $d \log p$ . For

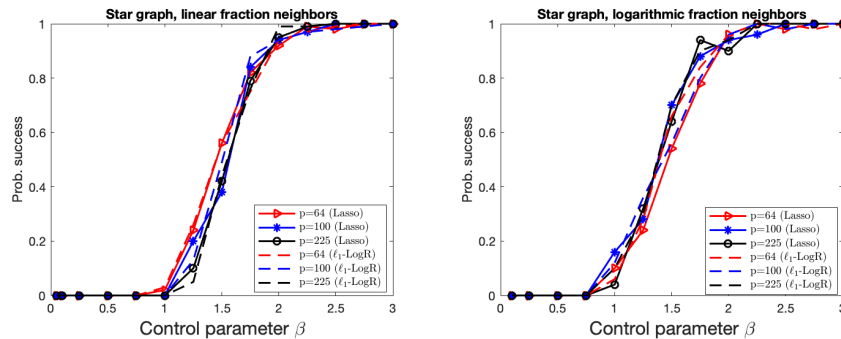


Figure 2: Success probability versus the control parameter  $\beta = \frac{n}{10d \log p}$  for Ising models on star-shaped graphs for attractive interactions  $\theta_{rt}^* = \frac{1.2}{\sqrt{d}}$  for all  $(r, t) \in E$ . Left: linear growth in degrees, i.e.,  $d = \lceil 0.1p \rceil$ ; Right: logarithmic growth in degrees, i.e.,  $d = \lceil \log p \rceil$ . In addition, the results of the  $\ell_1$ -LogR estimator [Ravikumar et al., 2010] are also shown. The results are averaged over 200 trials in all cases.

The results of RR graph and grid graph are shown in Fig. 1. In both cases, even for grid graph with many loops, using the Lasso estimator, all curves for different model sizes  $p$  line up with each other well, demonstrating that for a graph with fixed degree  $d$ , the ratio  $n/\log p$  controls the success or failure of the Ising model selection. Importantly, the behavior of the Lasso estimator is about the same as the  $\ell_1$ -LogR estimator.

Fig. 2 shows results for star-shaped graph whose maximum degree  $d$  is unbounded and grows as the dimension  $p$  grows. Two kinds of star-shaped graphs are considered by designating one node as the hub and connecting it to  $d < (p - 1)$  of its neighbors. Specifically, for linear sparsity, it is assumed that  $d = \lceil 0.1p \rceil$  while for logarithmic sparsity, we assume  $d = \lceil \log p \rceil$ . We use positive interactions and set the active interactions to be  $\theta_{rt}^* = \frac{1.2}{\sqrt{d}}$  for all  $(r, t) \in E$  as Ravikumar et al. [2010]. As depicted in Fig. 2, the results for growing degree of star-shaped graphs also line up with each other well, which is consistent with our theoretical analysis.

## 6 Conclusion

In this paper we have rigorously demonstrated that using the neighborhood-based Lasso, one can obtain consistent model selection for Ising models on any tree-like graph in the paramagnetic phase. The high-dimensional regime is applicable where both the number of nodes  $p$  and maximum node degree  $d$  grow as a function of the number of samples  $n$ . Remarkably, the obtained sample complexity for consistent model selection with Lasso has the same scaling as that of  $\ell_1$ -LogR [Ravikumar et al., 2010]. Experimental results on RR, star-shaped (both linear and logarithmic fraction neighbors), and even grid graphs with many loops, are consistent with the theoretical predictions. As future work, it is important to relax the assumption (A1) to consider both the general graphs and the low temperature

phases involving spontaneous symmetry breaking. Besides, it is very recently reported that a significant reduction of the sample complexity is possible by using non i.i.d. samples [Dutt et al., 2021]. As a result, investigating whether Lasso also works in the non i.i.d. case is also an interesting direction.

## Acknowledgement

We are thankful to Martin J. Wainwright and Pradeep Ravikumar for kindly providing their experimental settings of star-shaped graphs.

## References

- Alia Abbara, Yoshiyuki Kabashima, Tomoyuki Obuchi, and Yingying Xu. Learning performance in inverse Ising problems with sparse teacher couplings. *Journal of Statistical Mechanics: Theory and Experiment*, 2020(7):073402, 2020.
- Ludovica Bachschmid-Romano and Manfred Opper. A statistical physics approach to learning curves for the inverse Ising problem. *Journal of Statistical Mechanics: Theory and Experiment*, 2017(6):063406, 2017.
- José Bento and Andrea Montanari. Which graphical models are difficult to learn? In *Proceedings of the 22nd International Conference on Neural Information Processing Systems*, pages 1303–1311, 2009.
- Julian Besag. Statistical analysis of non-lattice data. *Journal of the Royal Statistical Society: Series D (The Statistician)*, 24(3):179–195, 1975.
- David R Brillinger. A generalized linear model with Gaussian regressor variables. In *A Festschrift for Erich L. Lehmann*, page 97–114. 1982.
- Aurélien Decelle and Federico Ricci-Tersenghi. Pseudolikelihood decimation algorithm improving the inference of the interaction network in a general class of Ising models. *Physical review letters*, 112(7):070603, 2014.
- Arkopal Dutt, Andrey Y Lokhov, Marc Vuffray, and Sidhant Misra. Exponential reduction in sample complexity with learning of Ising model dynamics. *arXiv preprint arXiv:2104.00995*, 2021.
- Andreas Engel and Christian Van den Broeck. *Statistical mechanics of learning*. Cambridge University Press, 2001.
- Martin Genzel. High-dimensional estimation of structured signals from non-linear observations with general convex loss functions. *IEEE Transactions on Information Theory*, 63(3):1601–1619, 2016.

- Robin Gomila. Logistic or linear? Estimating causal effects of experimental treatments on binary outcomes using regression analysis. *Journal of Experimental Psychology: General*, 150(4):700, 2021.
- Holger Höfling and Robert Tibshirani. Estimation of sparse binary pairwise Markov networks using pseudo-likelihoods. *Journal of Machine Learning Research*, 10(4), 2009.
- Ernst Ising. Beitrag zur theorie des ferromagnetismus. *Zeitschrift für Physik*, 31(1):253–258, 1925.
- Hilbert J. Kappen and Francisco de Borja Rodríguez. Efficient learning in Boltzmann machines using linear response theory. *Neural Computation*, 10(5):1137–1156, 1998.
- Daphne Koller and Nir Friedman. *Probabilistic graphical models: principles and techniques*. MIT press, 2009.
- Jeyashree Krishnan, Reza Torabi, Andreas Schuppert, and Edoardo Di Napoli. A modified Ising model of barabási–albert network with gene-type spins. *Journal of mathematical biology*, 81(3):769–798, 2020.
- Korbinian Liebl and Martin Zacharias. Accurate modeling of dna conformational flexibility by a multivariate Ising model. *Proceedings of the National Academy of Sciences*, 118(15), 2021.
- Andrey Y Lokhov, Marc Vuffray, Sidhant Misra, and Michael Chertkov. Optimal structure and parameter learning of Ising models. *Science advances*, 4(3):e1700791, 2018.
- Daniel Marbach, James C Costello, Robert Küffner, Nicole M Vega, Robert J Prill, Diogo M Camacho, Kyle R Allison, Manolis Kellis, James J Collins, and Gustavo Stolovitzky. Wisdom of crowds for robust gene network inference. *Nature methods*, 9(8):796–804, 2012.
- Julian J McAuley and Jure Leskovec. Learning to discover social circles in ego networks. volume 2012, pages 548–56. Citeseer, 2012.
- Nicolai Meinshausen, Peter Bühlmann, et al. High-dimensional graphs and variable selection with the lasso. *The annals of statistics*, 34(3):1436–1462, 2006.
- Xiangming Meng, Tomoyuki Obuchi, and Yoshiyuki Kabashima. Structure learning in inverse Ising problems using  $\ell_2$ -regularized linear estimator. *arXiv preprint arXiv:2008.08342*, 2020.
- Xiangming Meng, Tomoyuki Obuchi, and Yoshiyuki Kabashima. Ising model selection using  $\ell_1$ -regularized linear regression: A statistical mechanics analysis. *Advances in Neural Information Processing Systems*, 34, 2021.



- Marc Mezard and Andrea Montanari. *Information, physics, and computation*. Oxford University Press, 2009.
- Faruck Morcos, Andrea Pagnani, Bryan Lunt, Arianna Bertolino, Debora S Marks, Chris Sander, Riccardo Zecchina, José N Onuchic, Terence Hwa, and Martin Weigt. Direct-coupling analysis of residue coevolution captures native contacts across many protein families. *Proceedings of the National Academy of Sciences*, 108(49):E1293–E1301, 2011.
- H Chau Nguyen and Johannes Berg. Bethe–Peierls approximation and the inverse Ising problem. *Journal of Statistical Mechanics: Theory and Experiment*, 2012(03):P03004, 2012.
- Hidetoshi Nishimori. *Statistical physics of spin glasses and information processing: an introduction*. Number 111. Clarendon Press, 2001.
- Manfred Opper and David Saad. *Advanced mean field methods: Theory and practice*. MIT press, 2001.
- Matjaž Perc, Jillian J Jordan, David G Rand, Zhen Wang, Stefano Boccaletti, and Attila Szolnoki. Statistical physics of human cooperation. *Physics Reports*, 687:1–51, 2017.
- Yaniv Plan and Roman Vershynin. The generalized lasso with non-linear observations. *IEEE Transactions on information theory*, 62(3):1528–1537, 2016.
- Pradeep Ravikumar, Martin J Wainwright, John D Lafferty, et al. High-dimensional Ising model selection using  $\ell_1$ -regularized logistic regression. *The Annals of Statistics*, 38(3):1287–1319, 2010.
- Federico Ricci-Tersenghi. The Bethe approximation for solving the inverse Ising problem: a comparison with other inference methods. *Journal of Statistical Mechanics: Theory and Experiment*, 2012(08):P08015, 2012.
- R Tyrrell Rockafellar. *Convex analysis*, volume 36. Princeton university press, 1970.
- Adam J Rothman, Peter J Bickel, Elizaveta Levina, Ji Zhu, et al. Sparse permutation invariant covariance estimation. *Electronic Journal of Statistics*, 2:494–515, 2008.
- Narayana P Santhanam and Martin J Wainwright. Information-theoretic limits of selecting binary graphical models in high dimensions. *IEEE Transactions on Information Theory*, 58(7):4117–4134, 2012.
- Toshiyuki Tanaka. Mean-field theory of Boltzmann machine learning. *Physical Review E*, 58(2):2302, 1998.

- Christos Thrampoulidis, Ehsan Abbasi, and Babak Hassibi. Lasso with non-linear measurements is equivalent to one with linear measurements. *Advances in Neural Information Processing Systems*, 28:3420–3428, 2015.
- Robert Tibshirani. Regression shrinkage and selection via the lasso. *Journal of the Royal Statistical Society: Series B (Methodological)*, 58(1):267–288, 1996.
- Roman Vershynin. *High-dimensional probability: An introduction with applications in data science*, volume 47. Cambridge university press, 2018.
- Marc Vuffray, Sidhant Misra, Andrey Lokhov, and Michael Chertkov. Interaction screening: Efficient and sample-optimal learning of Ising models. In *Advances in Neural Information Processing Systems*, pages 2595–2603, 2016.
- Martin J. Wainwright. Sharp thresholds for high-dimensional and noisy sparsity recovery using  $\ell_1$ -constrained quadratic programming (lasso). *IEEE Transactions on Information Theory*, 55(5):2183–2202, 2009. doi: 10.1109/TIT.2009.2016018.
- Martin J Wainwright and Michael Irwin Jordan. *Graphical models, exponential families, and variational inference*. Now Publishers Inc, 2008.
- Martin J Wainwright, John D Lafferty, and Pradeep K Ravikumar. High-dimensional graphical model selection using  $\ell_1$ -regularized logistic regression. In *Advances in neural information processing systems*, pages 1465–1472, 2007.
- Yue Zhang, Weihong Guo, and Soumya Ray. On the consistency of feature selection with lasso for non-linear targets. In *International Conference on Machine Learning*, pages 183–191. PMLR, 2016.
- Peng Zhao and Bin Yu. On model selection consistency of lasso. *The Journal of Machine Learning Research*, 7:2541–2563, 2006.

## A Proof of Lemma 2

**Proof** The gradient of the square loss  $\ell(\theta_{\setminus r}; \mathfrak{X}_1^n)$  in (5) w.r.t.  $\theta_{\setminus r}$  reads

$$\nabla \ell(\theta_{\setminus r}; \mathfrak{X}_1^n) = \frac{1}{n} \sum_{i=1}^n x_{\setminus r}^{(i)} \left( x_r^{(i)} - \sum_{t \in V \setminus r} \theta_{rt} x_t^{(i)} \right). \quad (32)$$

After taking expectation of gradient  $\nabla \ell(\theta_{\setminus r}; \mathfrak{X}_1^n)$  over the distribution  $\mathbb{P}_{\theta^*}(x)$  and setting it to be zero, we obtain  $\mathbb{E}_{\theta^*}(\nabla \ell(\theta_{\setminus r}; \mathfrak{X}_1^n)) = 0$  in matrix form:

$$Q_r^* \theta_{\setminus r} = b, \quad (33)$$

where  $Q_r^* = \mathbb{E}_{\theta^*} (X_{\setminus r} X_r^T)$  is the covariance matrix of  $X_{\setminus r}$  and  $b = \mathbb{E}_{\theta^*} (X_{\setminus r} X_r)$ . The solution to (33), denoted as  $\tilde{\theta}_{\setminus r}^*$ , can be analytically obtained as  $\tilde{\theta}_{\setminus r}^* = (Q_r^*)^{-1} b$ . Next, we construct the full covariance matrix  $C = \mathbb{E}_{\theta^*} (X X^T)$  of all spins  $X$  as follows

$$C = \begin{bmatrix} 1 & b^T \\ b & Q_r^* \end{bmatrix}, \quad (34)$$

where  $X_r$  is indexed as the first variable in  $C$  without loss of generality. From the block matrix inversion lemma, the inverse covariance matrix can be computed as

$$C^{-1} = \begin{bmatrix} F_{11}^{-1} & -F_{11}^{-1} (\tilde{\theta}_{\setminus r}^*)^T \\ -\tilde{\theta}_{\setminus r}^* F_{11}^{-1} & F_{22}^{-1} \end{bmatrix}, \quad (35)$$

where

$$F_{11} = 1 - b^T (Q_r^*)^{-1} b, \quad (36)$$

$$F_{22} = Q_r^* - b b^T. \quad (37)$$

On the other hand, for sparse tree graph in the paramagnetic phase, the inverse covariance matrix  $C^{-1}$  can be computed from the Hessian of the Gibbs free energy [Abbara et al., 2020, Nguyen and Berg, 2012, Ricci-Tersenghi, 2012]. Specifically, each element of the covariance matrix  $C = \{C_{rt}\}_{r,t \in V}$  can be expressed as

$$C_{rt} = \mathbb{E}_{\theta^*} (x_r x_t) - \mathbb{E}_{\theta^*} (x_r) \mathbb{E}_{\theta^*} (x_t) = \frac{\partial^2 \log Z(\sigma)}{\partial \sigma_r \partial \sigma_t}, \quad (38)$$

where  $Z(\sigma) = \sum_x \mathbb{P}_{\theta^*} (x) e^{\sum_{s \in V} \sigma_s x_s}$  with  $\sigma = \{\sigma_s\}_{s \in V}$  and the assessment is carried out at  $\sigma = 0$ . In addition, for technical convenience we introduce the Gibbs free energy as

$$A(m) = \max_{\sigma} \{ \sigma^T m - \log Z(\sigma) \}. \quad (39)$$

The definition of (39) indicates that following two relations hold:

$$\frac{\partial m_r}{\partial \sigma_t} = \frac{\partial^2 \log Z(\sigma)}{\partial \sigma_r \partial \sigma_t} = C_{rt}, \quad (40)$$

$$\frac{\partial \sigma_r}{\partial m_t} = [C^{-1}]_{rt} = \frac{\partial^2 A(m)}{\partial m_r \partial m_t}, \quad (41)$$

where the evaluations are performed at  $\sigma = 0$  and  $m = \arg \min_m A(m)$  ( $= 0$  under the paramagnetic assumption). Consequently, the inverse covariance matrix of a tree graph  $G \in \mathcal{G}_{p,d}$  can be computed as [Abbara et al., 2020, Nguyen and Berg, 2012, Ricci-Tersenghi,

2012]

$$[C^{-1}]_{rt} = \left( \sum_{u \in \mathcal{N}(r)} \frac{1}{1 - \tanh^2(\theta_{ru}^*)} - d_r + 1 \right) \delta_{rt} - \frac{\tanh(\theta_{rt}^*)}{1 - \tanh^2(\theta_{rt}^*)} (1 - \delta_{rt}). \quad (42)$$

The two representations of  $C^{-1}$  in (35) and (42) are equivalent so that the corresponding elements should equal to each other. Thus, the following identities hold

$$\begin{cases} F_{11}^{-1} = \sum_{u \in \mathcal{N}(r)} \frac{1}{1 - \tanh^2(\theta_{ru}^*)} - d_r + 1, \\ \tilde{\theta}_{\setminus r}^* F_{11}^{-1} = \frac{\tanh(\theta_{\setminus r}^*)}{1 - \tanh^2(\theta_{\setminus r}^*)}, \end{cases} \quad (43)$$

where  $\tanh(\cdot)$  is applied element-wise. From (43), we obtain (16), which is a rescaled version of the true interactions. In particular, for RR graphs with constant coupling  $|\theta_{rt}^*| = \theta_0, \forall (r, t) \in E$  and  $d_r = d$ , substituting the results one can obtain,

$$\tilde{\theta}_{rt}^* = \begin{cases} \frac{\tanh(\theta_0) \text{sign}(\theta_{rt}^*)}{1 + (d-1) \tanh^2(\theta_0)} & \text{if } (r, t) \in E; \\ 0 & \text{otherwise.} \end{cases} \quad (44)$$

which completes the proof. ■

## B Proof of Lemma 3

**Proof** First,  $\mathbb{E}_{\theta^*} (Z_s^{(i)}) = 0$  can be readily obtained from Lemma 2. Thus, to prove  $\text{Var} (Z_s^{(i)}) \leq 1$ , it suffices to prove  $\mathbb{E}_{\theta^*} \left( (Z_s^{(i)})^2 \right) \leq 1$ . To this end, we introduce an auxiliary function

$$f_1(\theta_{\setminus r}) = \mathbb{E}_{\theta^*} \left( x_r^{(i)} - \sum_{t \in V \setminus r} \theta_t x_t^{(i)} \right)^2. \quad (45)$$

Thus we have  $\mathbb{E}_{\theta^*} \left( (Z_s^{(i)})^2 \right) = f_1(\tilde{\theta}_{\setminus r}^*)$ . The gradient vector can be computed as  $\nabla f_1(\theta_{\setminus r}) = 2\mathbb{E}_{\theta^*} (\nabla \ell(\theta_{\setminus r}; \mathfrak{X}_1^n))$ . Since  $\mathbb{E}_{\theta^*} (\nabla \ell(\tilde{\theta}_{\setminus r}^*; \mathfrak{X}_1^n)) = 0$  as shown in Lemma 2, we have  $\nabla f_1(\tilde{\theta}_{\setminus r}^*) = 0$ . Moreover, since  $\nabla^2 f_1(\theta_{\setminus r}) = 2\mathbb{E}_{\theta^*} (X_{\setminus r} X_r) \succ 0$ , we can conclude that  $f_1(\theta_{\setminus r})$  reaches

its minimum at  $\theta_{\setminus r} = \tilde{\theta}_{\setminus r}^*$ . As a result, we have

$$\begin{aligned}\mathbb{E}_{\theta^*} \left( \left( Z_s^{(i)} \right)^2 \right) &= f_1 \left( \theta_{\setminus r} = \tilde{\theta}_{\setminus r}^* \right) \\ &\leq f_1 \left( \theta_{\setminus r} = 0 \right) \\ &= \mathbb{E}_{\theta^*} \left( x_r^{(i)} \right)^2 \\ &= 1,\end{aligned}$$

where in the last line the fact that  $x_r^{(i)} \in \{-1, +1\}, \forall r \in V$  is used. Therefore, we obtain  $\text{Var} \left( Z_s^{(i)} \right) \leq 1$ .

Finally, recalling the result (16), we have

$$\begin{aligned}& \left( \sum_{u \in \mathcal{N}(r)} \frac{1}{1 - \tanh^2(\theta_{ru}^*)} - d_r + 1 \right) \sum_{t \in V \setminus r} \left| \tilde{\theta}_{rt}^* \right| \\ &= \sum_{t \in \mathcal{N}(r)} \frac{|\tanh(\theta_{rt}^*)|}{1 - \tanh^2(\theta_{rt}^*)} \\ &= \sum_{t \in \mathcal{N}(r)} \frac{|\tanh(\theta_{rt}^*)| + 1 - \tanh^2(\theta_{rt}^*) + \tanh^2(\theta_{rt}^*) - 1}{1 - \tanh^2(\theta_{rt}^*)} \\ &= -d_r + \sum_{t \in \mathcal{N}(r)} \frac{|\tanh(\theta_{rt}^*)| + 1 - \tanh^2(\theta_{rt}^*)}{1 - \tanh^2(\theta_{rt}^*)},\end{aligned}\tag{46}$$

To proceed, consider an auxiliary function  $f_2(x) = x + 1 - x^2, 0 \leq x \leq 1$ . Then it can be proved that  $1 \leq f_2(x) \leq \frac{5}{4}$ , so that from (46), we have

$$\sum_{t \in V \setminus r} \left| \tilde{\theta}_{rt}^* \right| \leq \frac{-d_r + \frac{5}{4} \sum_{u \in \mathcal{N}(r)} \frac{1}{1 - \tanh^2(\theta_{ru}^*)}}{\sum_{u \in \mathcal{N}(r)} \frac{1}{1 - \tanh^2(\theta_{ru}^*)} - d_r + 1}.\tag{47}$$

It can be easily checked that  $\sum_{u \in \mathcal{N}(r)} \frac{1}{1 - \tanh^2(\theta_{ru}^*)} \in [d_r, \infty)$ . We introduce another auxiliary function

$$f_3(x) = \frac{-d_r + \frac{5}{4}x}{x - d_r + 1}, x \in [d_r, \infty).\tag{48}$$

The first-order derivative of  $f_3(x)$  can be easily computed as

$$f_3'(x) = \frac{5 - d_r}{4(x - d_r + 1)^2}.\tag{49}$$

As a result,  $f_3'(x) > 0$  when  $d_r < 5$  and  $f_3'(x) < 0$  when  $d_r > 5$ . Consequently,

$$\max_{x \in [d_r, \infty)} f_3(x) = \begin{cases} \frac{5}{4} & d_r \leq 5 \\ \frac{d_r}{4} & d_r > 5 \end{cases} \quad (50)$$

Finally, combining the above results together yields

$$\left| Z_s^{(i)} \right| \leq \max \left\{ \frac{9}{4}, \frac{4 + d_r}{4} \right\} < d_r, \forall d_r \geq 3. \quad (51)$$

By definition, there is  $d_r \leq d$  so that  $\left| Z_s^{(i)} \right| \leq d$ , which completes the proof.  $\blacksquare$

## C Proof of Lemma 4

**Proof** According to Lemma 3, applying the Bernstein's inequality [Vershynin, 2018],  $\forall \eta > 0$  we have

$$\mathbb{P}(|W_s^n| > \eta) \leq 2 \exp \left( -\frac{\frac{1}{2}\eta^2 n}{1 + \frac{1}{3}d\eta} \right). \quad (52)$$

Similar to Vuffray et al. [2016], inverting the following relation

$$\xi = \frac{\frac{1}{2}\eta^2 n}{1 + \frac{1}{3}d\eta}, \quad (53)$$

and substituting the result in (52) yields

$$\mathbb{P} \left( |W_s^n| > \frac{1}{3} \left( u + \sqrt{u^2 + 18\frac{u}{d}} \right) \right) \leq 2 \exp(-\xi), \quad (54)$$

where  $u = \frac{\xi}{n}d$ . Suppose that  $n \geq \xi d^2$ , then  $u^2 = \frac{\xi^2}{n^2}d^2 \leq \frac{\xi}{n}$  while  $\frac{u}{d} = \frac{\xi}{n}$ . Consequently, we have

$$\begin{aligned} \frac{1}{3} \left( u + \sqrt{u^2 + 18\frac{u}{d}} \right) &\leq \frac{1}{3} \left( \sqrt{\frac{\xi}{n}} + \sqrt{\frac{\xi}{n} + 18\frac{\xi}{n}} \right) \\ &\leq \frac{1}{3} \left( \sqrt{\frac{\xi}{n}} + \sqrt{\frac{\xi}{n}} \sqrt{25} \right) \\ &= 2\sqrt{\frac{\xi}{n}}, \end{aligned}$$

where a relaxed result is obtained. Subsequently, we obtain an expression which is independent of  $d$ :

$$\mathbb{P} \left( |W_s^n| > 2\sqrt{\frac{\xi}{n}} \right) \leq 2 \exp(-\xi). \quad (55)$$

Setting  $\xi = (c+1) \log p$ , then if  $\lambda_n \geq \frac{4(2-\alpha)\sqrt{c+1}}{\alpha} \sqrt{\frac{\log p}{n}}$ , we have  $\frac{\alpha\lambda_n}{2(2-\alpha)} \geq 2\sqrt{\frac{\xi}{n}}$  so that

$$\mathbb{P} \left( \frac{2-\alpha}{\lambda_n} |W_s^n| > \frac{\alpha}{2} \right) \leq \mathbb{P} \left( |W_s^n| > 2\sqrt{\frac{\xi}{n}} \right) \leq 2 \exp(-(c+1) \log p). \quad (56)$$

Then, by using a union bound we have

$$\mathbb{P} \left( \frac{2-\alpha}{\lambda_n} \|W^n\|_\infty \geq \frac{\alpha}{2} \right) \leq 2 \exp(-c \log p). \quad (57)$$

As a result, when  $n \geq (c+1) d^2 \log p$ , as long as  $\lambda_n \geq \frac{4\sqrt{c+1}(2-\alpha)}{\alpha} \sqrt{\frac{\log p}{n}}$ , it is guaranteed that  $\mathbb{P} \left( \frac{2-\alpha}{\lambda_n} \|W^n\|_\infty \geq \frac{\alpha}{2} \right) \rightarrow 0$  at rate  $\exp(-c \log p)$  for some constant  $c > 0$ , which completes the proof.  $\blacksquare$

## D Proof of Lemma 5

**Proof** Using the method in Rothman et al. [2008], here the proof follows Ravikumar et al. [2010] but with some modifications. First, define a function  $\mathbb{R}^d \rightarrow \mathbb{R}$  as follows [Rothman et al., 2008]

$$G(u_S) := \ell \left( \tilde{\theta}_S^* + u_S; \mathfrak{X}_1^n \right) - \ell \left( \tilde{\theta}_S^*; \mathfrak{X}_1^n \right) + \lambda_n \left( \left\| \tilde{\theta}_S^* + u_S \right\|_1 - \left\| \tilde{\theta}_S^* \right\|_1 \right). \quad (58)$$

Note that  $G$  is a convex function w.r.t.  $u_S$ . Then  $\hat{u}_S = \hat{\theta}_S - \tilde{\theta}_S^*$  minimizes  $G$  according to the definition in (4). Moreover, it is easily seen that  $G(0) = 0$  so that  $G(\hat{u}_S) \leq 0$ . As described in Ravikumar et al. [2010], if we can show that there exists some radius  $B > 0$  and any  $u_S \in \mathbb{R}^d$  with  $\|u_S\|_2 = B$  satisfies  $G(u_S) > 0$ , then we can claim that  $\|\hat{u}_S\|_2 \leq B$  since otherwise one can always, by appropriately choosing  $t \in (0, 1]$ , find a convex combination  $t\hat{u}_S + (1-t)0$  which lies on the boundary of the ball with radius  $B$  and thus  $G(t\hat{u}_S + (1-t)0) \leq 0$ , leading to contradiction. Consequently, it suffices to establish the strict positivity of  $G$  on the boundary of a ball with radius  $B = M\lambda_n\sqrt{d}$ , where  $M > 0$  is one parameter to choose later.

Specifically, let  $u_S \in \mathbb{R}^d$  be an arbitrary vector with  $\|u_S\|_2 = B$ . Expanding the

quadratic form  $\ell\left(\tilde{\theta}_S^* + u_S; \mathfrak{X}_1^n\right)$ , we have

$$G(u_S) = -(W_S^n)^T u_S + u_S^T Q_{SS}^n u_S + \lambda_n \left( \left\| \tilde{\theta}_S^* + u_S \right\|_1 - \left\| \tilde{\theta}_S^* \right\|_1 \right), \quad (59)$$

where  $W_S^n$  is the sub-vector of  $W^n = -\nabla \ell\left(\tilde{\theta}^*; \mathfrak{X}_1^n\right)$ , and  $Q_{SS}^n$  is the sub-matrix of the sample covariance matrix  $Q^n$ . The expression (59) is simpler than the counterpart in Ravikumar et al. [2010] which is obtained from the Taylor series expansion of the non-quadratic loss function and thus its quadratic term is dependent on  $\theta$ . To proceed, we investigate the bounds of the three terms in the right hand side (RHS) of (59), respectively.

Since  $\|u_S\|_1 \leq \sqrt{d} \|u_S\|_2$  and  $\|W_S^n\|_\infty \leq \frac{\lambda_n}{2}$ , the first term is bounded as

$$\left| -(W_S^n)^T u_S \right| \leq \|W_S^n\|_\infty \|u_S\|_1 \leq \|W_S^n\|_\infty \sqrt{d} \|u_S\|_2 \leq \left( \lambda_n \sqrt{d} \right)^2 \frac{M}{2}. \quad (60)$$

The third term is bounded as

$$\lambda_n \left( \left\| \tilde{\theta}_S^* + u_S \right\|_1 - \left\| \tilde{\theta}_S^* \right\|_1 \right) \geq -\lambda_n \|u_S\|_1 \geq -\lambda_n \sqrt{d} \|u_S\|_2 = -M \left( \lambda_n \sqrt{d} \right)^2. \quad (61)$$

The remaining middle Hessian term in RHS of (59) is, different from Ravikumar et al. [2010], quite simple due to the square loss function:

$$\begin{aligned} u_S^T Q_{SS}^n u_S &\geq \|u_S\|_2^2 \Lambda_{\min} \left( \frac{1}{n} \sum_i x_S^{(i)} \left( x_S^{(i)} \right)^T \right) \\ &= \|u_S\|_2^2 \Lambda_{\min} (Q_{SS}^*) \\ &\geq C_{\min} M^2 \left( \lambda_n \sqrt{d} \right)^2, \end{aligned} \quad (62)$$

where the last inequality comes from the dependency condition  $\Lambda_{\min} (Q_{SS}^*) \geq C_{\min}$  in (8). In contrast to Ravikumar et al. [2010], there is no need to control the additional spectral norm.

Combining the three bounds (60) - (62) together with (59), we obtain that

$$G(u_S) \geq \left( \lambda_n \sqrt{d} \right)^2 \left\{ -\frac{M}{2} + C_{\min} M^2 - M \right\}. \quad (63)$$

It can be easily verified from (63) that  $G(u_S)$  is strictly positive when we choose  $M = \frac{3}{C_{\min}}$ . Consequently, as long as  $\|W^n\|_\infty \leq \frac{\lambda_n}{2}$ , we are guaranteed that  $\|\hat{u}_S\|_2 \leq M \lambda_n \sqrt{d} = \frac{3 \lambda_n \sqrt{d}}{C_{\min}}$ , which completes the proof.  $\blacksquare$



## D.1 Proof of Proposition 1

Before the proof, we first introduce the following Lemma.

**Lemma 8** *Consider a RR graph with uniform coupling strength  $\theta_0$  and constant node degree  $d$ . Under the paramagnetic assumption, the covariance between  $x_r$  and  $x_t$  can be calculated to be  $\mathbb{E}_{\theta^*} \{x_r x_t\} - \mathbb{E}_{\theta^*} \{x_r\} \mathbb{E}_{\theta^*} \{x_t\} = \tanh^l(\theta_0)$ , where  $l$  is the distance between node  $s$  and node  $t$  in the graph.*

**Proof** The Ising model on a RR graph is analytically solvable by Bethe approximation. Specifically, the corresponding belief propagation (BP) equation can be written as follows [Mezard and Montanari, 2009]

$$m_{r \rightarrow t} = \tanh \left( \sum_{k \in \mathcal{N}(r) \setminus t} \tanh^{-1}(\tanh(\theta_0) m_{k \rightarrow r}) \right). \quad (64)$$

where  $m_{r \rightarrow t}$  is the message from node  $r$  to node  $t$ . The spontaneous magnetization for the node  $r \in V$  is assessed as

$$m_r = \tanh \left( \sum_{t \in \mathcal{N}(r)} \tanh^{-1}(\tanh(\theta_0) m_{t \rightarrow r}) \right). \quad (65)$$

Due to the uniformity of RR graphs, these equations are reduced to

$$m_c = \tanh \left( (d-1) \tanh^{-1}(\tanh(\theta_0) m_c) \right), \quad (66)$$

$$m = \tanh \left( d \tanh^{-1}(\tanh(\theta_0) m) \right), \quad (67)$$

where we set  $m_{r \rightarrow t} := m_c$  and  $m_r := m$  for all directed edges  $r \rightarrow t$  and all nodes  $r \in V$ .

Suppose that  $x = (x_r)_{r=1}^p$  is subject to a Hamiltonian  $H(x) = -\sum_{s \neq t} \theta_{st}^* x_s x_t$ . For this, we define the Helmholtz free energy as

$$F(\xi) = -\ln \left( \sum_x \exp \left( -H(x) + \sum_{r=1}^p \xi_r x_r \right) \right). \quad (68)$$

Using  $F(\xi)$ , one can evaluate the expectation of  $x$  as

$$m_r := \mathbb{E}_{\theta^*} \{x_r\} = - \left. \frac{\partial F(\xi)}{\partial \xi_r} \right|_{\xi=0} = \frac{\sum_x x_r \exp(-H(x))}{\sum_x \exp(-H(x))}. \quad (69)$$

In addition, the covariance of  $x_r$  and  $x_t$  can be computed as

$$\mathbb{E}_{\theta^*} \{x_r x_t\} - \mathbb{E}_{\theta^*} \{x_r\} \mathbb{E}_{\theta^*} \{x_t\} \quad (70)$$

$$\begin{aligned}
&= \left. \frac{\partial \mathbb{E}_{\theta^*} \{x_r\}}{\partial \xi_t} \right|_{\xi=0} \\
&= \frac{\sum_x x_r x_t \exp(-H(x))}{\sum_x \exp(-H(x))} - \frac{\sum_x x_r \exp(-H(x))}{\sum_x \exp(-H(x))} \cdot \frac{\sum_x x_t \exp(-H(x))}{\sum_x \exp(-H(x))}, \quad (71)
\end{aligned}$$

where the last equation is termed the *linear response relation*.

Suppose that node  $r$  is placed at the distance of  $l$  from node  $t$ . A remarkable property of tree graphs, including RR graph, is that a unique path is defined between two arbitrary nodes. This indicates that the linear response relation (71) can be evaluated by the chain rule of partial derivative using messages of belief propagation as

$$\mathbb{E}_{\theta^*} \{x_r x_t\} - \mathbb{E}_{\theta^*} \{x_r\} \mathbb{E}_{\theta^*} \{x_t\} = \left. \frac{\partial m_r}{\partial \xi_t} \right|_{\xi=0} = (1 - m^2) \left( \frac{\tanh(\theta_0) (1 - m_c^2)}{1 - \tanh^2(\theta_0) m_c^2} \right)^l. \quad (72)$$

Under the paramagnetic assumption, there are  $m = 0$  and  $m_c = 0$ . As a result, one obtain

$$\mathbb{E}_{\theta^*} \{x_r x_t\} - \mathbb{E}_{\theta^*} \{x_r\} \mathbb{E}_{\theta^*} \{x_t\} = \tanh^l(\theta_0). \quad (73)$$

■

Now we are ready for the proof. First, we consider the *dependency condition*. In the case of RR graph, the distances between any two different nodes in  $S := \{(r, t) \mid t \in \mathcal{N}(r)\}$  are 2. Consequently, according to Lemma 8, all the off-diagonal elements in sub-matrix  $Q_{SS}^*$  equal to  $\tanh^2 \theta_0$  and all the diagonal elements equal to 1, i.e.,

$$Q_{SS}^* = \begin{bmatrix} 1 & \tanh^2 \theta_0 & \tanh^2 \theta_0 & \cdots & \tanh^2 \theta_0 \\ \tanh^2 \theta_0 & 1 & \tanh^2 \theta_0 & \vdots & \tanh^2 \theta_0 \\ \tanh^2 \theta_0 & \tanh^2 \theta_0 & \ddots & \tanh^2 \theta_0 & \vdots \\ \vdots & \cdots & \tanh^2 \theta_0 & 1 & \tanh^2 \theta_0 \\ \tanh^2 \theta_0 & \tanh^2 \theta_0 & \cdots & \tanh^2 \theta_0 & 1 \end{bmatrix}_{d \times d}. \quad (74)$$

It can be analytically computed that  $Q_{SS}^*$  has two different eigenvalues: one is  $1 + (d - 1) \tanh^2 \theta_0$  and the other is  $1 - \tanh^2 \theta_0$  with multiplicity  $(d - 1)$ . Consequently,  $Q_{SS}^*$  has bounded eigenvalue and we explicitly obtain the result of  $C_{\min}$  as

$$\Lambda_{\min}(Q_{SS}^*) = 1 - \tanh^2 \theta_0 := C_{\min}. \quad (75)$$

Then, we prove that the *incoherence condition* also satisfies. From (74), the inverse matrix  $(Q_{SS}^*)^{-1}$  can be analytically computed as

$$(Q_{SS}^*)^{-1} = \begin{bmatrix} a & b & b & \cdots & b \\ b & a & b & \vdots & b \\ b & b & \cdots & b & \vdots \\ \vdots & \cdots & b & a & b \\ b & b & \cdots & b & a \end{bmatrix}_{d \times d}, \quad (76)$$

where

$$a = \frac{1 + (d-2) \tanh^2 \theta_0}{(1 - \tanh^2 \theta_0) (1 + (d-1) \tanh^2 \theta_0)}, \quad (77)$$

$$b = -\frac{\tanh^2 \theta_0}{(1 - \tanh^2 \theta_0) (1 + (d-1) \tanh^2 \theta_0)}. \quad (78)$$

Then, by definition of  $\| \| Q_{S^c S}^* (Q_{SS}^*)^{-1} \| \|_\infty$ , according to Lemma 8, it is achieved for  $r \in S^c$  where  $r$  belongs to the nearest neighbors of the nodes in  $S$ . Specifically, in that case, the elements in the row in  $Q_{S^c S}^*$  associated with node  $r \in S^c$  can only take two different values: one element is  $\tanh \theta_0$  and the other  $(d-1)$  elements are  $\tanh^3 \theta_0$ . Then, from (76), after some algebra, it can be calculated that

$$\| \| Q_{S^c S}^* (Q_{SS}^*)^{-1} \| \|_\infty = \tanh \theta_0 := 1 - \alpha, \quad (79)$$

where we obtain an analytical result  $\alpha := 1 - \tanh \theta_0 \in (0, 1]$ , which completes the proof.